 Ingeniería e Industria	DESIGN AND OPTIMIZATION OF RIGID SAILS TO REDUCE SHIPPING RELATED GREENHOUSE GAS EMISSIONS	Computer science
RESEARCH ARTICLE	Carlos Reca, Fernando J. Aguilar, Antonio Giménez, Manuel A. Aguilar	1203.26 Simulation

DESIGN AND OPTIMIZATION OF RIGID SAILS TO REDUCE SHIPPING RELATED GREENHOUSE GAS EMISSIONS

Carlos Reca, Fernando J. Aguilar, Antonio Giménez y Manuel A. Aguilar
 Universidad de Almería. Dpto. de Ingeniería. Carretera de Sacramento, s/n - 04120 La Cañada de San Urbano, Almería (España).

Received: 27/jun/2022 • Reviewing: 30/jun/2022 • Accepted: 14/sep/2022 | DOI: <https://doi.org/10.6036/10630>


To cite this article: RECA, Carlos; AGUILAR, Fernando J.; GIMÉNEZ, Antonio; AGUILAR, Manuel A. METHODOLOGICAL PROPOSAL FOR THE SELECTION AND ANALYSIS OF THE PERFORMANCE

RIGID SAILS CONSIDERING PRE-STALL AND POST-STALL AERODYNAMIC CONDITIONS. DYNA, January-February 2022, vol. 98, n.1, pp. 78-85. DOI: <https://doi.org/10.6036/10630>

ABSTRACT:

The shipping industry is increasingly considering the issues of "green shipping" and "zero-emission shipping", which are closely related to reducing the consumption of fossil fuels to mitigate its environmental impact. In this way, the use of renewable energies is increasingly perceived as part of the energy mix, with the use of rigid sails (wind energy) being one of the tested alternatives as auxiliary propulsion systems. This work studied the fluid-mechanical optimization of the airfoil that defines the cross section geometry of the rigid sail. A methodology was developed to obtain the aerodynamic coefficients of the rigid sail for any position of the sail with respect to the wind depending on the tested airfoil. Once the aerodynamic coefficients were modeled for several angles of attack, the thrust and overturning components generated by the sail force on the boat were computed from before and after airfoil stalling predictive models of the aerodynamic coefficients. From the obtained results, the following two main conclusions can be stated. i) The use of the sail in post-stall conditions for higher angles of incidence (from approximately 90°) substantially improved the thrust generated on the boat. For the case of small incidence angles, it is recommended to set the sail at an angle of attack less than the airfoil stall. ii) Within the symmetrical four-digit NACA series, the symmetrical NACA 0015 airfoil turned out to be the best choice for geometrically defining the rigid sail cross section, as it provided the highest possible thrust while minimizing the overturning force.

Key Words: rigid sails, wind powered, airfoil, aerodynamic coefficients, CFD

 Ingeniería e Industria	DESIGN AND OPTIMIZATION OF RIGID SAILS TO REDUCE SHIPPING RELATED GREENHOUSE GAS EMISSIONS	Computer science
RESEARCH ARTICLE	Carlos Reca, Fernando J. Aguilar, Antonio Giménez, Manuel A. Aguilar	1203.26 Simulation

1. INTRODUCTION

Maritime transport is, by far, the most cost-effective way to move goods around the world. However, maritime transport also emits around 940 million tons of CO₂ annually, being responsible for about 2.5% of global greenhouse gas (GHG) emissions [1]. In this sense, the shipping industry is increasingly considering the issues of "green shipping" and "zero-emissions shipping", which are closely related to reducing the consumption of fossil fuels to mitigate its environmental impact. This is the strategy outlined by the European Union through a recent plan to reduce shipping related GHG emissions [2].

Throughout the history of maritime navigation, vessels have been modifying their propulsion methods with the arrival of new technologies that allowed them to be bigger and faster, now focusing on guaranteeing the environmental sustainability of vessels by reducing, and even eliminating, the emission of GHG that contribute to global warming [3]. In particular, the use of renewable energies is increasingly perceived as part of the energy mix, with the use of rigid sails (wind energy) being one of the most tested alternatives as auxiliary propulsion systems [4].

Based on the need to reduce both fossil fuel consumption and atmospheric emissions across the shipping sector, several technologies have been developed or are currently in the development phase. Rigid sails is one of those technologies, being extensively researched and tested in the 1980s. There has now been a resurgence of interest in this technology that clearly aligns with green shipping [4]. In this regards, the reader can find a review of various wind propulsion technologies available in the market in [5], most of them using the same principle as sailing to produce thrust.

But what lies behind rigid sail propulsion technology? As we commented above, rigid sail, usually made of carbon fibers or metal, is a variation of conventional soft sail inspired by airplane wings design (thin airfoil theory; e.g. [7]). The advantage of rigid sails over traditional sails stems from its variable camber aerodynamic shape (airfoil shape), thus providing more lift and a higher lift to drag ratio than traditional soft sails [8]. Contrary to aircraft, the objective of a good rigid sail profile installed on a boat is to improve its aerodynamic performance by maximizing the combination of lift and drag forces in the forward direction of the vessel in order to maximize thrust (Figure 1). Note that for a certain angle of attack (AOA), that is the angle formed by the chord of the airfoil and the direction of the relative wind (Figure 2), the airfoil geometry causes a difference in air velocity around it, thus resulting in a combination of higher and lower pressure around the airfoil that generates the lift.

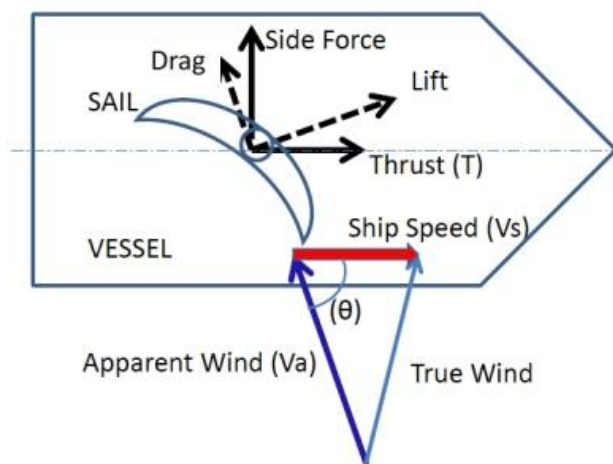



Figure 1: Apparent wind, ship speed, thrust, and main wind-derived forces acting on a rigid sail [6]

 Ingeniería e Industria	DESIGN AND OPTIMIZATION OF RIGID SAILS TO REDUCE SHIPPING RELATED GREENHOUSE GAS EMISSIONS	Computer science
RESEARCH ARTICLE	Carlos Reca, Fernando J. Aguilar, Antonio Giménez, Manuel A. Aguilar	1203.26 Simulation

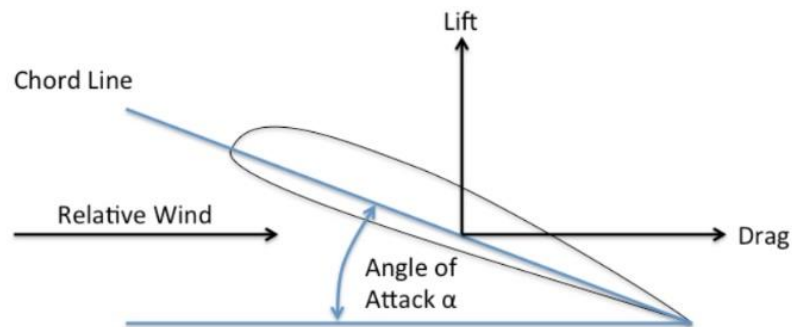


Figure 2: Graphical representation (cross section) of angle of attack for a certain airfoil

The fundamental difference between the different rigid sails is the profile they present, the most common being the use of symmetrical airfoils from the aeronautical industry. The use of symmetric airfoils is due to their stability against sudden changes in wind direction, unlike non-symmetric airfoils. In other words, in this type of profiles a change in the direction of the wind does not generate a sudden variation in the force generated that could destabilize the boat. However, this stability is gained at the cost of losing thrust in the boat.

After this brief introduction, it is time to set the objectives of this work. It aims to study the fluid-mechanical optimization of the airfoil that defines the geometry of a rigid sail. For this, a study of different existing symmetrical airfoils (symmetrical four-digit NACA series; <http://airfoiltools.com/>) and the involved aerodynamic principles was carried out. In addition, the behavior of the wind in navigation was also analyzed. Once determined the airfoils to be studied and the wind conditions that act on the sail, a methodology was developed to obtain the aerodynamic coefficients of the rigid sail for any position of the sail with respect to the wind.

2. MATERIALS AND METHODS

2.1 AIRFOILS SELECTED

The family of airfoils selected to carry out the study was the symmetric four-digit NACA series (<http://airfoiltools.com/>). This series presents a geometry that is easy to trace based on the so-called thickness parameter. The use of these profiles in aviation is carried out with relatively small thicknesses (around 12% thickness with respect to the chord) to achieve good lift values. If the thickness of the profile take values above 30%, approximately, it will present high drag values and lower lift values than profiles with less thickness. If, on the other hand, the thickness of the airfoil is reduced below 8%, the lift value also decreases, approaching that of a flat plate. In either of these two cases, the airfoil would lack of interest to be used in rigid sails. It should be noted that although the combination of lift and drag forces are responsible for the thrust in rigid sails, it is also true that the lift component will present a greater relevance in most of the possible angles of incidence of the wind.

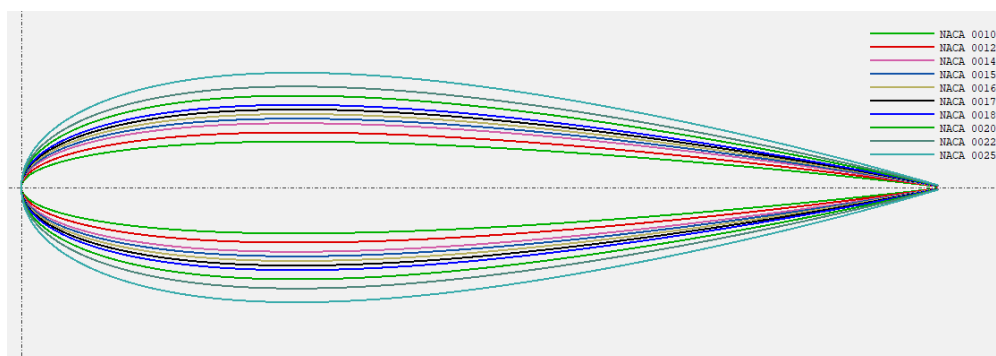



Figure 3: Plots of the different NACA airfoils tested in this work

	DESIGN AND OPTIMIZATION OF RIGID SAILS TO REDUCE SHIPPING RELATED GREENHOUSE GAS EMISSIONS	Computer science
RESEARCH ARTICLE	Carlos Reca, Fernando J. Aguilar, Antonio Giménez, Manuel A. Aguilar	1203.26 Simulation

Therefore, the NACA profiles to be selected should fall within this interval of thickness parameter. In addition, two more airfoils were tested. The first one was NACA 0015, recommended in a study undertaken by the University of Southampton [9]. The second one was NACA 0025, proposed by the Spanish company Bound4Blue [10]. The plots of all the airfoils tested in this study are shown in Figure 3.

2.2 INITIAL CONDITIONS

A rigid sail, contrarily to an airfoil for aviation, must adapt the angle of attack according to the angle of incidence of the apparent wind at any moment in order to maximize the thrust force at that particular time. Therefore, it would not make sense to analyze only the angles of attack up to the stall point, since the predominant aerodynamic force in that range would be the lift force. That is why it is necessary to study the rigid sail beyond that angle, where the contribution of the drag force becomes greater and greater until it reaches its maximum at 90°. Furthermore, it should be considered that the rigid sail is symmetrical and, consequently, the behavior of the airfoil for positive and negative angles of attack is the same. This fact makes it possible to reduce the range of angles to be studied. Considering these two phenomena, the study range set for angles of attack varies from 0° to 90°.

On the other hand, if we analyze the climatic working conditions, the apparent wind speed has to be taken into account. In order to determine the apparent wind speed, it is necessary to compute the true wind speed as well as the speed of the vessel.

For the determination of the true wind, the Beaufort scale can be used. This shows that the most favorable condition for the rigid sail without incurring storm consequences is to work at level 5, which means working with a wind speed between 8 and 10.7 m/s. In order to carry out this study, it was decided to work on the safe side by establishing a wind speed of 8 m/s.

Regarding the speed of the vessel, and trying to develop an airfoil applicable to all types of vessels, this speed was considered sufficiently small enough to rule it out. Therefore, the relative wind speed used in this study will correspond to the true wind speed as defined above.

In addition to the wind speed, a kinematic wind viscosity of $1.51 \cdot 10^{-5}$ m²/s, a wind density of 1.225 kg/m³ and a unit value chord will be considered.

2.3 METHODOLOGY PROPOSED TO OBTAIN THE AERODYNAMIC COEFFICIENTS

The aerodynamic forces developed by a given airfoil depend on its geometry, density, air speed and dimensionless coefficients that depend on the angle of attack at each instant of time. In consequence, the aerodynamic lift and drag forces can be defined mathematically as shown in equations 1 and 2.

$$F_L = \frac{1}{2} \cdot \rho \cdot V^2 \cdot A \cdot C_L \quad (1)$$

$$F_D = \frac{1}{2} \cdot \rho \cdot V^2 \cdot A \cdot C_D \quad (2)$$


Where A is the area projected in a plane perpendicular to the direction of flow. However, in the case of thin bodies, as it occurs in aeronautics, the plan area or wing area is used. CL and CD are the dimensionless aerodynamic coefficients for lift and drag, while the term $1/2 \cdot \rho \cdot V^2$ corresponds to the dynamic pressure.

In order to calculate the forces developed by the airfoil, once the rest of the variables are known, it is necessary to compute the value of their coefficients for each one of the angles of attack that we are interested in. That means that it is necessary to calculate the values of the coefficients before and after the stall, as indicated in section 2.2.

For the calculation of these coefficients, it is proposed to divide the problem into two blocks: i) before stall aerodynamic coefficients and ii) after stall aerodynamic coefficients.

In this sense, the aerodynamic drag and lift coefficients prior to the airfoil stalling were obtained using the XFLR5 computational fluid dynamics (CFD) software. Since a discrete number of data was obtained depending on the chosen step, the data was fitted to a third degree polynomial function.

On the other hand, and due to the fact that CFD software does not properly provide the coefficients beyond the stall point, the use of experimental models instead is proposed in this methodology. The two experimental fluid-mechanical models evaluated in this paper

	DESIGN AND OPTIMIZATION OF RIGID SAILS TO REDUCE SHIPPING RELATED GREENHOUSE GAS EMISSIONS	Computer science
RESEARCH ARTICLE	Carlos Reca, Fernando J. Aguilar, Antonio Giménez, Manuel A. Aguilar	1203.26 Simulation

were the Viterna model [11] and the Aerodas model [12]. These models were originally devised to estimate the power output of large horizontal axis wind turbines working under low speed conditions and high angles of attack.

From combining these two models, it is possible to simulate the behavior of the airfoil for a wide range of angles of attack (i.e., before and after stall angles).

2.4 METHODOLOGY PROPOSED TO OBTAIN THE THRUST AND OVERTURNING COEFFICIENTS

Once the aerodynamic coefficients have been obtained, it is essential to know the component that favors the movement of the vessel and the component that produces an overturning moment in it. Rigid sails can be oriented in two different ways. First, the angle formed between the chord of the rigid sail and the longitudinal axis of the boat (β) is less than the angle formed between the apparent wind direction and the boat's direction of travel (γ) (Figure 4, left). Second, the rigid sail chord angle is greater than the angle of incidence of the apparent wind direction (Figure 4, right).

Note that positioning the sail so that the angle of incidence of the apparent wind is closer to the longitudinal axis of the boat than the angle of the sail would not allow forces to be generated in the forward direction of the boat if the angle of incidence of the wind is less than 90° . If, on the other hand, the angle of incidence were greater than 90° , only the drag force would contribute to the forward thrust of the boat. Moreover, in the case of placing the sail closer to the longitudinal axis of the boat than the angle of incidence of the wind, the longitudinal component of the vessel's lift force would allow the vessel to be propelled for angles of incidence of the wind up to 90° . Finally, if the wind were blowing from the stern of the ship, both forces would contribute to the ship's propulsion.

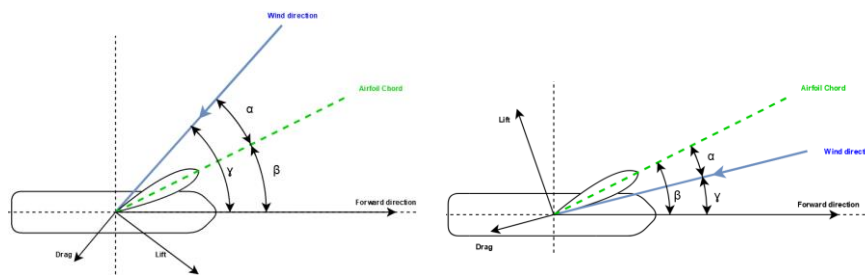


Figure 4: Different windward orientations of the rigid sail

From this simple analysis, we can deduce that, to correctly use a rigid sail, it is necessary to always position the sail at an angle less than the angle of incidence of the apparent wind with respect to the direction of movement of the boat. In this regards, decomposing the forces generated in the sail under this orientation, the thrust force, F_x , and the overturning force, F_y , can be obtained as shown in equations 3 and 4.

$$F_x = F_L \cdot \sin(\gamma) - F_D \cdot \cos(\gamma) \quad (3)$$


$$F_y = F_L \cdot \cos(\gamma) + F_D \cdot \sin(\gamma) \quad (4)$$

Where F_L and F_D refers to the lift and drag forces defined in equations 1 and 2, respectively. If the thrust and overturning forces are defined in the same way as the lift and drag forces, all the variables relating to the rigid sail geometry and wind conditions can be simplified. Therefore, equations 3 and 4 can be expressed in terms of dimensionless coefficients C_x and C_y (for thrust and overturning forces, respectively) as follows:

$$C_x = C_L \cdot \sin(\gamma) - C_D \cdot \cos(\gamma) \quad (5)$$

$$C_y = C_L \cdot \cos(\gamma) + C_D \cdot \sin(\gamma) \quad (6)$$

In this way, the aerodynamic coefficients for the thrust of a vessel can be obtained independently of the fluid conditions and the geometry of the driving rigid sail. Therefore, once the lift and drag coefficients are computed for a given airfoil, the coefficients of the

	DESIGN AND OPTIMIZATION OF RIGID SAILS TO REDUCE SHIPPING RELATED GREENHOUSE GAS EMISSIONS	Computer science
RESEARCH ARTICLE	Carlos Reca, Fernando J. Aguilar, Antonio Giménez, Manuel A. Aguilar	1203.26 Simulation

characteristic thrust and overturning forces for that airfoil could be calculated and, subsequently, the positioning of the sail that best satisfy the thrust requirements can be deduced.

To calculate the maximum value of the thrust coefficient and its associated overturning coefficient, a MATLAB program was developed to, through an iterative process, calculate the angle of attack required to maximize the value of the thrust coefficient for each angle of incidence of the apparent wind. It used the third degree polynomial model fitted to XFLR5 software outputs, in the case of before stall angles of attack or the experimental model for after stall angles of attack. In other words, the program analyses for each angle of incidence the position in which the rigid sail should be placed in order to propel the vessel as effectively as possible.

Once all the angles of incidence have been analyzed, the program stores the triad of data (angle of attack, thrust coefficient and overturning coefficient) for all the angles of incidence studied. The iterative operation of the program for the calculation of the output triad can be appreciated in Figure 5.

```

gamma ← 0
while(gamma ≤ 180°)
  alpha ← 0
  while(alpha ≤ 90°)
    if(alpha ≤ airfoil stalling angle)
      Calculation of CL and CD as a function of α for the prestall data fitting model
    else
      Calculation of CL and CD as a function of α for the poststall model
    end_if
    Calculation of Cx and Cy as a function of the calculated aerodynamic coefficients
    if(Cx > Cx stored for previous alpha angles)
      Storage of the coefficients Cx and Cy, as well as the gamma and alpha angles
    end_if
    alpha ← alpha + 1
  end_while
  gamma ← gamma + 1
end_while


```

Figure 5: Pseudocode fragment of the program for calculating the thrust and overturning coefficients

2.5 BRIEF SUMMARY OF THE PROPOSED METHODOLOGY

The methodology proposed in the previous sections is summarised in Figure 6. As can be observed, the first step is to select the airfoil and its aerodynamic working conditions (air density and air speed). From this information, the pre-stall aerodynamic drag and lift coefficients are calculated by using XFLR5, a CFD software specifically devised to be used in the aeronautics field. This software generates a series of discrete data, which are later fitted to a third degree polynomial model, thus obtaining the pre-stall model of the airfoil under analysis.

Regarding the post-stall aerodynamic coefficients, two experimental models (Viterna or Aerodas) are tested to compute the lift and drag coefficients of the airfoil. It is worth noting that the use of the Aerodas model requires knowledge of some values of the pre-stall coefficients, unlike the Viterna model. That is the reason why it is indicated by an arrow with a dashed line in Figure 6. Once the models of the aerodynamic lift and drag coefficients before and after stall have been obtained, an iterative approach is applied to determine the angle of attack that maximizes the value of the thrust coefficient for each angle of incidence of the wind. In this way, the values of the thrust and overturning coefficients are computed for each angle of incidence of the relative wind.

	DESIGN AND OPTIMIZATION OF RIGID SAILS TO REDUCE SHIPPING RELATED GREENHOUSE GAS EMISSIONS	Computer science
RESEARCH ARTICLE	Carlos Reca, Fernando J. Aguilar, Antonio Giménez, Manuel A. Aguilar	1203.26 Simulation

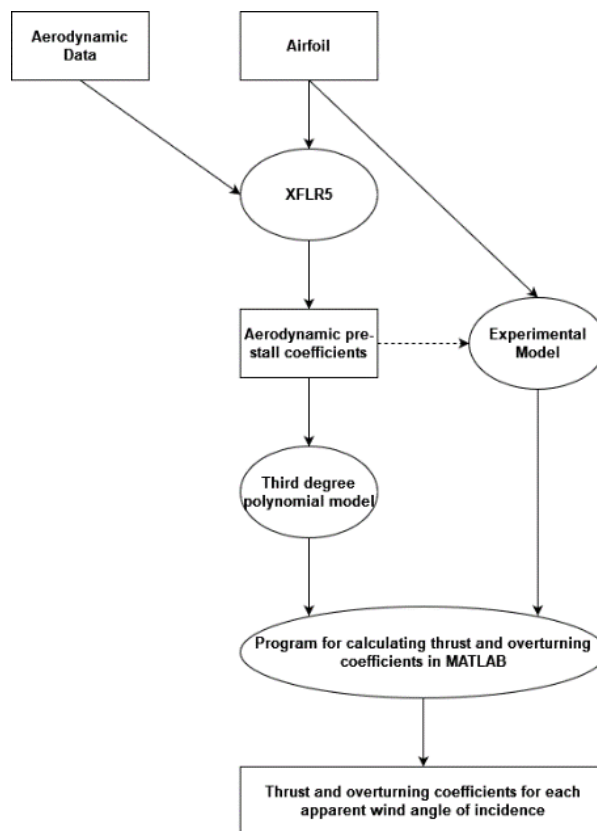


Figure 6: Schematic diagram of the methodology to obtain the thrust and overturning coefficients


3. STUDY CASE

3.1. CHARACTERISTICS OF THE STUDIED MARITIME ROUTE

In order to analyze the performance of a geometrically defined rigid sail with the optimum airfoil, one of the cases proposed by the company Bound4Blue on its website was used. The case chosen is that of an oil tanker covering a maritime route between Rotterdam and New Orleans [13]. The oil tanker and maritime route characteristics are listed in Tables I and II, respectively.

Characteristic	Value
Length	157 m
Beam	23.5 m
Draft	9.6 m
Deadweight	19350 t
Engine power at maximum load	5110 kW
Service speed	13 kt (6.7m/s)

Table I: Oil tanker characteristics

 Ingeniería e Industria	DESIGN AND OPTIMIZATION OF RIGID SAILS TO REDUCE SHIPPING RELATED GREENHOUSE GAS EMISSIONS	Computer science
	RESEARCH ARTICLE	Carlos Reca, Fernando J. Aguilar, Antonio Giménez, Manuel A. Aguilar

Characteristic	Value
Maritime route	Rotterdam - New Orleans
Distance	4726 NM (8758 km)
Travel time	15 days
Fuel consumption per trip	210.2 t

Table II: Maritime route characteristics

3.2. COMPUTATION OF RIGID SAIL PERFORMANCE

The performance of the rigid sail depends on the generated thrust force. The greater the thrust force, the greater the work generated by the wind and, therefore, the less fossil fuel consumption. Thus, in order to calculate the rigid sail performance it is necessary to know, firstly, the work that the rigid sail is capable of developing and, secondly, the work that the boat engine assumes under normal conditions. The relationship between the two workloads determines the performance of a particular rigid sail.

The work that a sail is capable of exerting over a given distance will be the product of the thrust force multiplied by the distance of the maritime route (d_{route} in equation 7). Remember that for the same environmental conditions, the thrust force depends only on the area of the rigid sail selected and the thrust coefficient that the airfoil of the rigid sail is capable of developing. Therefore, the thrust coefficient selected must be the one corresponding to the most probable angle of incidence of the wind for a given sea route.

$$W_{rigid\ sail} = F_x \cdot d_{route} \quad (7)$$

The work developed by the engine depends on the mass of fuel consumed together with its calorific value multiplied by the overall efficiency of the engine. In addition to this, the energy losses that occur in the transmission system and, subsequently, in the propeller must be taken into account. The product of all these variables indicates the actual work performed by the conventional propulsion system for a particular maritime route (equation 8).

$$W_{engine} = m_c \cdot H \cdot \eta_m \cdot \eta_{st} \cdot \eta_h \quad (8)$$

Where m_c is the mass of fuel consumed on a given route, H is the calorific value of the fuel, η_m is the overall engine efficiency, η_{st} is the efficiency of the drive system, and η_h is the propeller efficiency. The values used for these performances are shown in Table III.


Performance	Value
Engine efficiency (η_m)	0.50
Drive system efficiency (η_{st})	0.94
Propeller efficiency (η_h)	0.61

Table III: Propulsion system performances

Once the workloads are calculated, the efficiency of the rigid sail is calculated as the ratio between the work done by the rigid sail and the work of the conventional engine, as can be seen in equation 9.

$$\eta_{rigid\ sail} = \frac{W_{rigid\ sail}}{W_{engine}} \quad (9)$$

Finally, the economic savings per unit length travelled can be calculated using the equation 10.

	DESIGN AND OPTIMIZATION OF RIGID SAILS TO REDUCE SHIPPING RELATED GREENHOUSE GAS EMISSIONS	Computer science
RESEARCH ARTICLE	Carlos Reca, Fernando J. Aguilar, Antonio Giménez, Manuel A. Aguilar	1203.26 Simulation

$$\Delta CE_{c,km} = \frac{m_c}{d_{route}} \cdot \eta_{rigid\ sail} \cdot P_c \quad (10)$$

Where $\Delta CE_{c,km}$ is the variation in fuel cost per km and p_c the fuel price.

4. RESULTS AND DISCUSSION

4.1. PRE-STALL LIFT AND DRAG COEFFICIENTS

The values of the pre-stall aerodynamic drag and lift coefficients of each of the airfoils tested, obtained from the XFLR5 software, were fitted to third degree polynomial models, as mentioned previously. A specific example is shown below using the airfoil NACA 0015 (Figures 7 and 8).

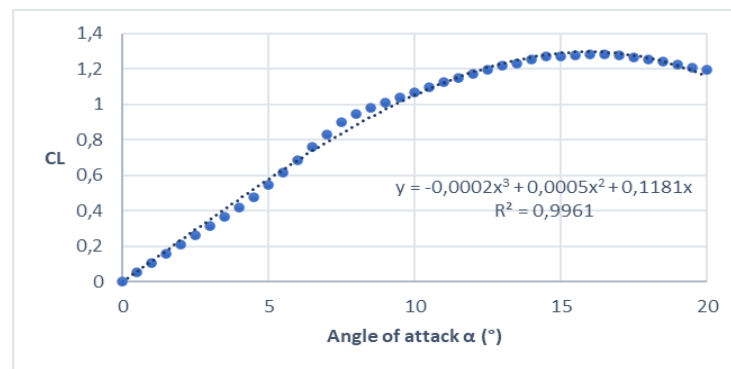


Figure 7: Pre-stall lift coefficients for NACA 0015 airfoil

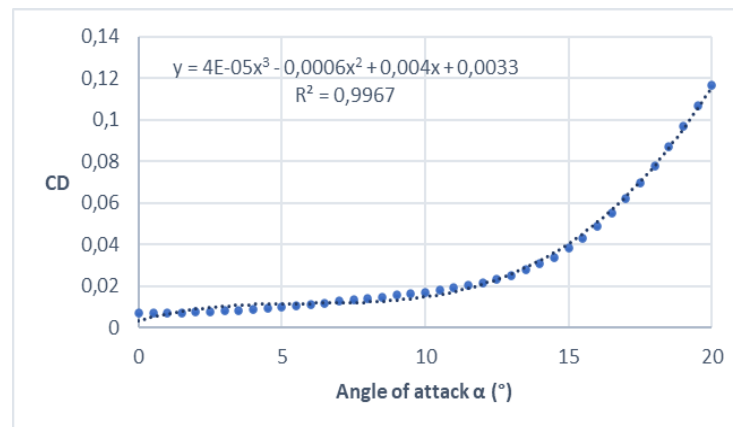


Figure 8: Pre-stall drag coefficients for NACA 0015 airfoil

4.2. POST-STALL EXPERIMENTAL MODEL

In order to determine the most suitable experimental model for obtaining the post-stall aerodynamic coefficients, a MATLAB program was coded. The result of the comparison between the Viterna and Aerodas models is presented in Figures 9 and 10 for lift and drag coefficients, respectively. They represent in blue the pre-stall aerodynamic coefficients obtained by XFLR5, in yellow the post-stall coefficients corresponding to the Viterna model, and in orange those corresponding to the Aerodas model.

As can be appreciated, both models had a similar behavior in predicting the reduction in the value of the lift coefficient from about 45°. The main difference between the two models concerning this coefficient turned out to be within the interval from the stall point to 45°. In the case of the Viterna model, lift would be reduced progressively in this area, whereas in the case of the Aerodas model, once the stall point is reached, there is an important reduction in the lift coefficient followed by a gradual increase in the lift coefficient up to 41°, when it begins to decrease progressively. As far as the drag coefficient is concerned, both models performed similar.

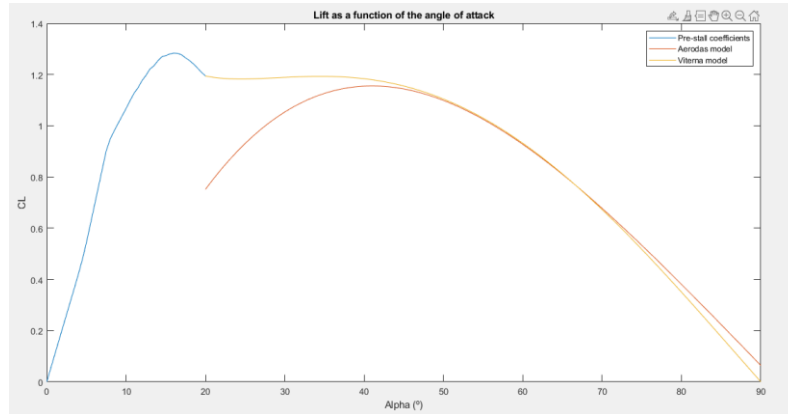


Figure 9: Comparison of the lift coefficient between experimental models for NACA 0015 airfoil

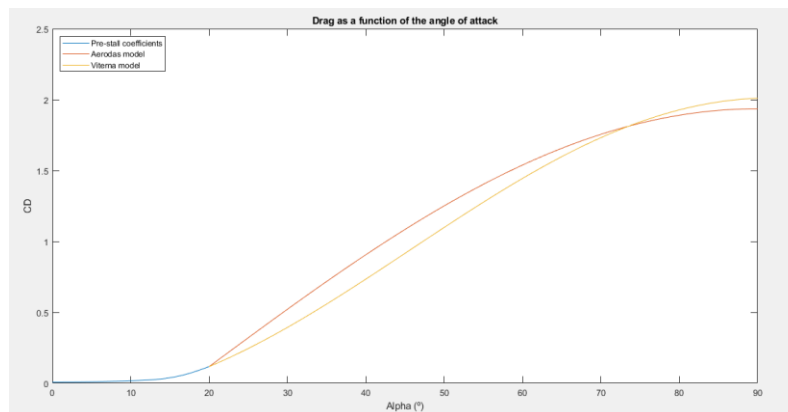


Figure 10: Comparison of the drag coefficient between experimental models for NACA 0015 airfoil

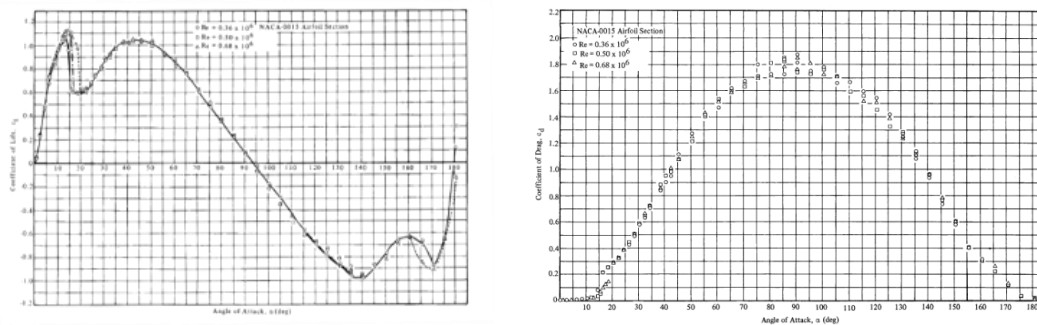



Figure 11: Aerodynamic lift (right) and drag (left) coefficients obtained in wind tunnel tests for NACA 0015 airfoil [14]

	DESIGN AND OPTIMIZATION OF RIGID SAILS TO REDUCE SHIPPING RELATED GREENHOUSE GAS EMISSIONS	Computer science
RESEARCH ARTICLE	Carlos Reca, Fernando J. Aguilar, Antonio Giménez, Manuel A. Aguilar	1203.26 Simulation

If the trends obtained with both models are compared with the plots obtained from the wind tunnel tests, as shown in Figure 11, it can be stated that the model that best adjusted to the real behaviour of the coefficients was the Aerodas model, being able to better reproduce the reduction in the lift coefficient once the airfoil stall occurs.

4.3. IMPORTANCE OF THE UTILIZATION OF THE RIGID SAIL IN POST-STALL CONDITIONS

The calculation of the maximum value of the thrust coefficient for each angle of incidence of the apparent wind is obtained by adjusting the angle of attack, as noted in previous sections. Depending on the value of the angle of attack, two possibilities can be considered: (i) working only with angles of attack up to the stall angle, or (ii) additionally including the post-stall angles of attack.

To visualize the impact of each possibility on the thrust coefficient, the maximum values of the thrust coefficient were calculated by taking into account both alternatives. To illustrate the results, polar diagrams are used (Figure 12). In these diagrams, the angle corresponds to the angle of incidence of the apparent wind, while the magnitude represents the maximum value of the thrust coefficient (C_x).

As can be seen, when the wind is coming from the front of the boat (bow), the C_x values in both cases are the same, indicating that it is more beneficial to trim the sail with pre-stall angles of attack. However, when the apparent wind comes from the back of the boat, it is more interesting to work with angles of attack greater than the stall point. In these cases, there is a progressive increase in thrust until reaching its maximum value when the angle of incidence of the wind is 180° . In the case of working with pre-stall angles of attack, the thrust value decreases progressively until reaching its minimum value at 180° . This demonstrates the importance of considering the post-stall conditions in the analysis of thrust coefficients.

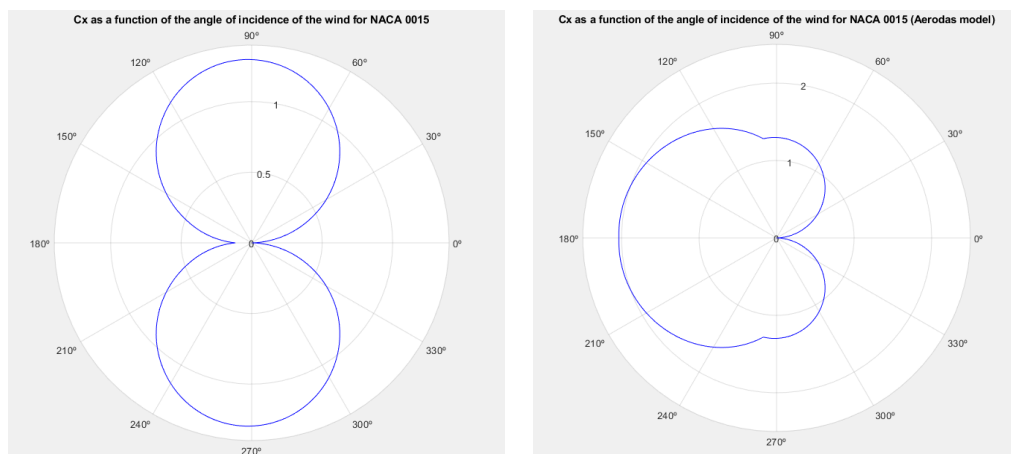



Figure 12: Thrust coefficient (C_x) as a function of the angle of incidence of the relative wind for NACA 0015 without considering (left) and considering (right) the post-stall conditions

4.4. THRUST AND OVERTURNING COEFFICIENTS. SELECTION OF THE OPTIMAL AIRFOIL

Applying the methodology described in the section "Materials and methods", the values of the thrust (C_x) and overturning (C_y) coefficients can be obtained. As an example, the value of these coefficients for the airfoil NACA 0015 in relation to the angle of incidence of the wind is shown in Figure 13. In addition, the angle of attack associated with each angle of incidence of the wind is represented in Figure 14.

Looking at these figures, it can be seen how the airfoils work in two completely different ways depending on the angle of incidence of the apparent wind. Firstly, when the apparent wind comes from the front of the boat (i.e., from an angle of incidence of 0° to the angle of change of region, between 90° and 100° depending on the airfoil), it is possible to make out how the sail adopts practically constant angles of attack of around 15° . This arrangement of the rigid sail in relation to the wind makes it possible to generate thrust forces from very small angles of incidence starting at 1° . At these first working angles, the overturning coefficient reaches its highest value, becoming the most important coefficient and then gradually decreasing. From angles of incidence of about 45° , the thrust coefficient will be higher than the overturning coefficient. It should be noted that, throughout this region, lift would be the aerodynamic force of the airfoil that makes the greatest contribution to the thrust and overturning forces.

	DESIGN AND OPTIMIZATION OF RIGID SAILS TO REDUCE SHIPPING RELATED GREENHOUSE GAS EMISSIONS	Computer science
RESEARCH ARTICLE	Carlos Reca, Fernando J. Aguilar, Antonio Giménez, Manuel A. Aguilar	1203.26 Simulation

When the angle of incidence of the wind occurs beyond the angle of change of region, the angle of attack should be drastically increased beyond the angle of stall to achieve higher thrust, and then the angle of attack must be progressively increased as the angle of incidence is higher. This finding has two important effects: firstly, the thrust coefficient increases more pronouncedly and, secondly, the overturning coefficient experiences an instantaneous increase, which is accompanied by a gradual decrease in the overturning coefficient. Both effects are because, in this region, the drag force begins to become more relevant than the lift force due to the gradual increase in the angle of attack.

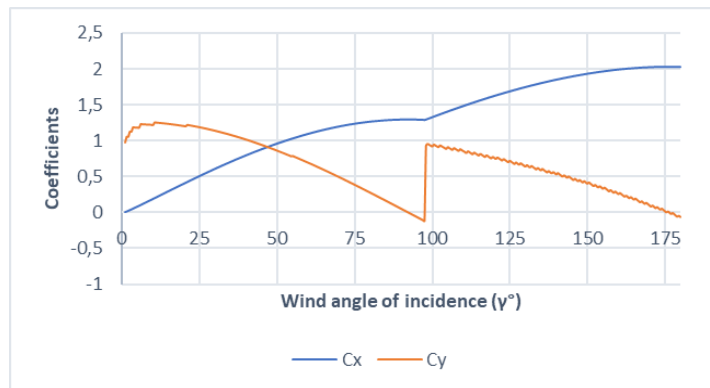


Figure 13: Thrust and overturning coefficients for NACA 0015 airfoil depending on wind angle of incidence (γ)

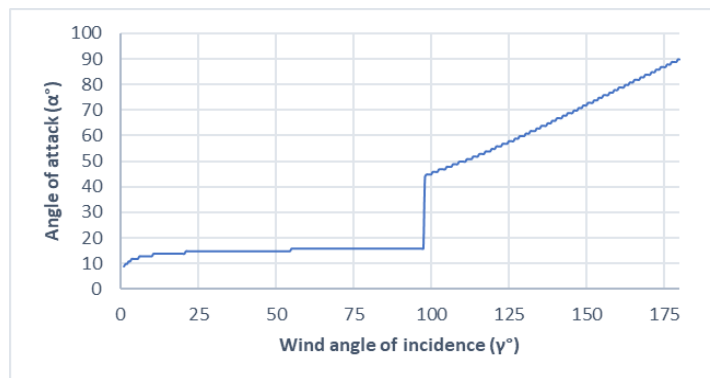



Figure 14: Angle of attack (α) as a function of wind angle of incidence (γ) for NACA 0015

Based on the thrust and overturning coefficients obtained for each airfoil, a comparison of the average behavior of the airfoils was undertaken in order to determine which of them generates a higher vessel's thrust supposing that all the angles of incidence are equiprobable. As can be seen in Figure 15, the highest average thrust values are generated by airfoils with thicknesses similar to NACA 0014. As the thickness of the airfoils increases, the average thrust coefficients become smaller and smaller. When it decreases below 12%, the average coefficients are drastically reduced.

	DESIGN AND OPTIMIZATION OF RIGID SAILS TO REDUCE SHIPPING RELATED GREENHOUSE GAS EMISSIONS	Computer science
RESEARCH ARTICLE	Carlos Reca, Fernando J. Aguilar, Antonio Giménez, Manuel A. Aguilar	1203.26 Simulation

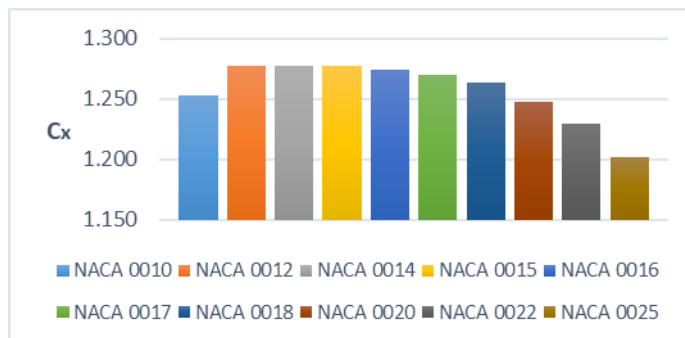


Figure 15: Average thrust coefficient (C_x value) for each airfoil analyzed

Regarding the value of the overturning coefficient, there is a clear decreasing trend as the airfoil thickness increases (Figure 16).

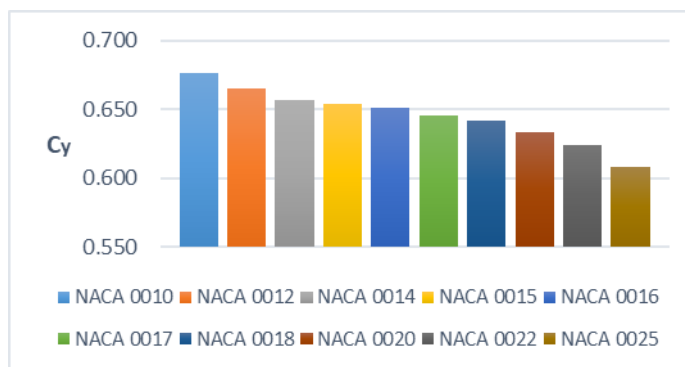


Figure 16: Average overturning coefficient (C_y value) for each airfoil analyzed


Taking all these considerations into account, it seems reasonable to consider that the NACA 0015 airfoil would be the best candidate, as it offers a high thrust coefficient while its overturning coefficient is lower than airfoils with similar thrust.

4.5. RESULTS RELATED TO THE STUDY CASE

This section shows the efficiencies for the case study presented in section three that could potentially be achieved if the rigid sail with the optimal geometry obtained in this work were installed. As indicated in section 3.1, these performances were obtained for a tanker with a diesel engine propulsion system operating on the Rotterdam-New Orleans route. The airfoil used is NACA 0015, applying the average of the computed thrust coefficients.

As can be seen in Figure 17, when the sail area is small (40 m²), the rigid sail performance is very low for any apparent wind speed. As the sail area increases, the differences between the performances obtained at different wind speeds for the same sail area increase. On the other hand, when wind speeds are lower than 6 m/s, the performances obtained are very low and a very high sail area would be necessary. However, when wind speeds are higher, a small increase in wind speed produces substantial improvements in performance. In the case of a wind speed of 8 m/s, it can be achieved an efficiency of 6.18% for a surface of 360 m², increasing to up to 13.91% in the case of a wind speed of 12 m/s. It is worth noting that for the first case mentioned the company Bound4Blue points to a yield of 5.86% by using a rigid sail with the same sail area and a NACA 0025 airfoil.

Finally, Figure 18 shows the economic savings in euros per kilometer for each combination of wind and rigid sail area. As can be seen, the trend is equivalent to that of the performance. Thus, in the case of installing a 360 m² rigid sail and considering a wind speed of 8 m/s, the total saving on the maritime route would be 7149 euros.

	DESIGN AND OPTIMIZATION OF RIGID SAILS TO REDUCE SHIPPING RELATED GREENHOUSE GAS EMISSIONS	Computer science
RESEARCH ARTICLE	Carlos Reca, Fernando J. Aguilar, Antonio Giménez, Manuel A. Aguilar	1203.26 Simulation

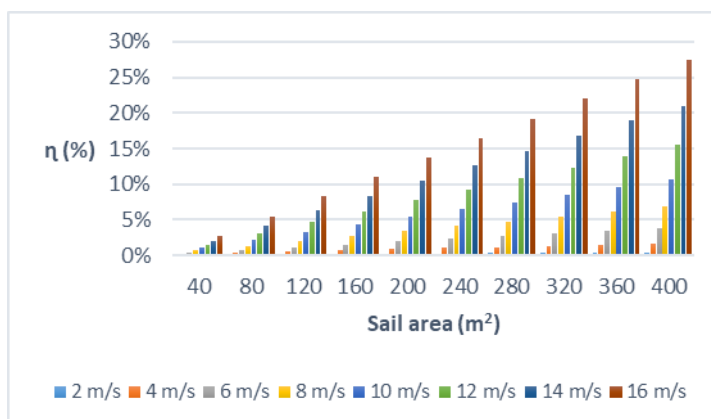


Figure 17: Rigid sail performance as a function of wind speed for each sail area

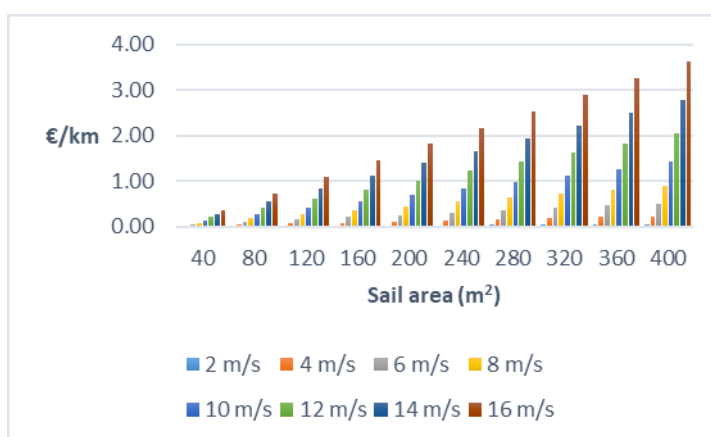



Figure 18: Economic savings depending on wind speed for each sail area

5. CONCLUSIONS

From the results obtained in this work, the following conclusions can be stated:

- i) It has been proved that the use of the sail in post-stall conditions for high angles of incidence, i.e. from approximately 90°, substantially improves the thrust generated on the boat. However, and for lower angles of incidence, it is more interesting to arrange the sail at an angle of attack less than the airfoil stall. Working in these two different ways, and depending on the apparent wind incidence angle, allows optimizing the thrust that the rigid sail is capable of producing. In this way, the proposed method, based on combining specific computational fluid dynamics tools of the aeronautical field with the calculation of aerodynamic coefficients from experimental models linked to applied engineering in the wind turbine sector, turned out to be an effective way to analyze and optimizing the thrust and overturning forces resulting from a wide range of incidence angles of the wind on the rigid sail.
- ii) Within the symmetrical four-digit NACA series, the NACA 0015 airfoil showed to be the best choice for geometrically defining the rigid sail cross section, as it provides the highest possible thrust while minimizing the overturning force.
- iii) Applying the method developed in this work, we have simulated the performance of the previously described case study (oil tanker travelling from Rotterdam to New Orleans) when using a rigid sail with a sail area of 360 m² and NACA 0015 airfoil. For an average wind speed of 8 m/s, the rigid sail performance computed by the simulation took a value of 6.18%, a slightly higher value than the one provided by the Bound4Blue company of 5.86%. To increase the performance of the wind propulsion system, it would be necessary to increase the sail surface available, for example, by installing several rigid sails. This shows that the use of rigid sails can derive in a reduction in fuel consumption, improving the efficiency of the propulsion systems of most ships and, therefore, reducing shipping related GHG emissions.

	DESIGN AND OPTIMIZATION OF RIGID SAILS TO REDUCE SHIPPING RELATED GREENHOUSE GAS EMISSIONS	Computer science
RESEARCH ARTICLE	Carlos Reca, Fernando J. Aguilar, Antonio Giménez, Manuel A. Aguilar	1203.26 Simulation

REFERENCES

- Smith, T., Jalkanen, J.P., Anderson, B.A., Corbett, J.J., Faber, J., Hanayama, S., O’Keeffe, E., Parker, S., Johansson, L., Aldous, L., Raucci, C., Traut, M., Ettinger, S., Nelissen, D., Lee, D.S., Ng, S., Agrawal, A., Winebrake, J.J., Hoen, M., Chesworth, S., Pandey, A.: Third IMO GHG Study 2014: Executive Summary and Final Report. , London, UK (2015).
- European Commission: Reducing emissions from the shipping sector, https://ec.europa.eu/clima/eu-action/transport-emissions-reducing-emissions-shipping-sector_es.
- Serra, P., Fancello, G.: Towards the IMO’s GHG Goals: A Critical Overview of the Perspectives and Challenges of the Main Options for Decarbonizing International Shipping. Sustainability. 12, 3220 (2020). <https://doi.org/10.3390/SU12083220>.
- Atkinson, G., Nguyen, H., Binns, J.: Considerations regarding the use of rigid sails on modern powered ships. Cogent Eng. 5, 1–20 (2018). <https://doi.org/10.1080/23311916.2018.1543564>.
- Rutkowski, G.: Study of Green Shipping Technologies - Harnessing Wind, Waves and Solar Power in New Generation Marine Propulsion Systems. TransNav, Int. J. Mar. Navig. Saf. Sea Transp. 10, 627–632 (2017). <https://doi.org/10.12716/1001.10.04.12>.
- Kazuyuki, O., Kiyoshi, U., Kanai, A.: Huge Hard Wing Sails for the Propulsor of Next Generation Sailing Vessel. In: Second International Symposium on Marine Propulsors smp’11. pp. 1–5. , Hamburg (2011).
- Kaushik, M.: Thin Airfoil Theory. In: Kaushik, M. (ed.) Theoretical and Experimental Aerodynamics. pp. 127–144. Springer Singapore, Singapore (2019). https://doi.org/10.1007/978-981-13-1678-4_5.
- Ariffin, N.I.B., Hannan, M.A.: Wingsail technology as a sustainable alternative to fossil fuel. IOP Conf. Ser. Mater. Sci. Eng. 788, 12062 (2020). <https://doi.org/10.1088/1757-899X/788/1/012062>.
- Burden, A., Lloyd, T., Mockler, S., Mortola, L., Shin, B., Smith, B., Hearn, G.E.: Concept Design of a Fast Sail Assisted Feeder Container Ship. , Global Energy Economics and Climate Protection Report , Southampton (2009).
- Wingsail Technology | Wind-Assisted Propulsion System for vessels | bound4blue, <https://bound4blue.com/en/wingsail>.
- Viterna, L.A., Janetzke, D.C.: Theoretical and experimental power from large horizontal-axis wind turbines. , Cleveland, USA (1982). <https://doi.org/10.2172/6763041>.
- Spera, D.A.: Models of Lift and Drag Coeffi cients of Stalled and Unstalled Airfoils in Wind Turbines and Wind Tunnels. , Cleveland (2008).
- Bound4Blue: Velas rígidas, <https://bound4blue.com/es/velas-rigidas>, last accessed 2020/05/05.
- E. Sheldai, R., C. Klimas, P.: Aerodynamic Characteristics of seven symmetrical airfoil sections through 180-degree angle of attack. National Technical Information Service U. S. Department of Commerce, Albuquerque (1981).

6. ACKNOWLEDGMENTS

This work takes part of the general research lines promoted by the Agrifood Campus of International Excellence ceiA3, Spain (<http://www.ceia3.es/en>). The authors would like to thank also to the INGEGRAF association.